

D.W. MA^{1,2,✉}
Z.Z. YE¹
Y.S. YANG²

Photoluminescent analysis of $\text{Zn}_{1-x}\text{Cd}_x\text{O}$ alloys

¹ State Key Laboratory of Silicon Materials, Zhejiang University, Hangzhou 310027, P.R. China
² RCDAMP, Department of Physics, Pusan National University, Pusan 609-735, South Korea

Received: 1 June 2005/Revised version: 16 August 2005
Published online: 12 October 2005 • © Springer-Verlag 2005

ABSTRACT The photoluminescent (PL) spectra of $\text{Zn}_{1-x}\text{Cd}_x\text{O}$ ($0 \leq x \leq 0.53$) alloy films were obtained successfully. A new explanation from the viewpoint of band structure is brought forward to comprehend the PL nature of the alloy films. According to this explanation, the near-band-energy emissions of the $\text{Zn}_{1-x}\text{Cd}_x\text{O}$ ($x > 0$) films are caused by the radiative transitions between the $\text{Zn}4s$ – $\text{Cd}5s$ hybrid level and the $\text{O}2p$ level, and the broadenings of the two levels are responsible for the gradually increased line width of the PL peak of the film; $\text{Zn}3d$ and $\text{Cd}4d$ orbital levels have great effects on the band-gap variations of the alloys. In addition, a quadratic equation is put forward to depict the relationship between the band gaps E_g of the alloys and their Cd contents x , i.e. $E_g(x) = 3.30 - 1.22x + 1.26x^2$ ($0 \leq x \leq 0.53$).

PACS 78.55.-m; 78.55.Et; 81.15.Cd

1 Introduction

As an analogy to GaN, the II–VI compound semiconductor ZnO has a wide direct band gap of 3.3 eV and an even larger excitonic binding energy of 60 meV than that of GaN (25 meV), which makes it possible to fabricate ZnO-based blue and ultraviolet (UV) light-emitting diodes (LEDs) and laser diodes (LDs) [1, 2].

ZnCdO is also regarded as an ideal material for ZnO-based devices. Being alloyed with CdO, which has a narrower direct band gap of 2.3 eV, the band gap of ZnO can be red shifted to the blue- and even green-light spectral ranges. Moreover, considering the similarities of Zn and Cd in their radii and other basic properties, a proper incorporation of CdO into ZnO is very useful for the fabrication of $\text{ZnO}/\text{Zn}_{1-x}\text{Cd}_x\text{O}$ heterojunctions or superlattices, which are the key elements in ZnO-based LED and LD devices [3]. However, most reports on $\text{Zn}_{1-x}\text{Cd}_x\text{O}$ alloy films were not satisfactory due to the coexistence of multiphase or polycrystalline states without preferred orientations, and little is known about the photoluminescent (PL) properties of the $\text{Zn}_{1-x}\text{Cd}_x\text{O}$ alloys [4–9].

We have successfully grown highly (002)-preferred $\text{Zn}_{1-x}\text{Cd}_x\text{O}$ alloy films with the maximum Cd content of

53 at.% and obtained their PL spectra for the first time. Moreover, the PL phenomena of the $\text{Zn}_{1-x}\text{Cd}_x\text{O}$ alloy films are discussed in detail from a new viewpoint of band structure, which is undoubtedly of great importance for a deep understanding of the PL nature, the fundamental physics and the potential applications of the $\text{Zn}_{1-x}\text{Cd}_x\text{O}$ and other ternary alloys. Also, a quantitative quadratic equation between the band gaps E_g of the alloys and their Cd contents x is put forward, which can guide us to select different $\text{Zn}_{1-x}\text{Cd}_x\text{O}$ alloy compositions to satisfy the needs of different band gaps, as will be discussed later in this paper.

2 Experimental

A series of $\text{Zn}_{1-x}\text{Cd}_x\text{O}$ ($0 \leq x \leq 1.0$) films were deposited on Si(111) substrates by a dc reactive magnetron sputtering method. The sputtering targets with different ratios of Zn to Cd were prepared using Zn and Cd metals with a high purity of 99.999%. The deposition chamber was evacuated to a base pressure of 10^{-3} Pa. High-purity (99.995%) argon and oxygen were used as sputtering and reactive gases. The specific flux of argon and oxygen was controlled at a ratio of $\text{Ar} : \text{O}_2 \sim 1 : 4$ and the total pressure maintained at 4.0 Pa. The sputtering current and sputtering voltage were 200 mA and 200 V, respectively. The deposition time was 30 min for each sample. The crystal structures of the samples were investigated by X-ray diffraction (XRD) measurements, where a $\text{Cu } K_\alpha$ ($\lambda = 0.154056$ nm) source was used. The PL spectra of the films were measured at 12 K by using a He–Cd laser (325 nm). The film compositions were determined by X-ray photoemission spectroscopy (XPS) measurements, as was discussed elsewhere [10]; the compositions x mentioned below all denote the measured film compositions.

3 Results and discussion

Figure 1 shows the XRD patterns of $\text{Zn}_{1-x}\text{Cd}_x\text{O}$ ($0 \leq x \leq 1$) films. For the samples with $x \leq 0.53$, only (002) Bragg peaks characteristic of the hexagonal wurtzite ZnO are observed, indicating single-phase states with nearly complete c -axis preferred orientations for the films. Further increasing the Cd content to $x = 0.77$, an obvious phase separation of cubic CdO is detected. Moreover, it is evident that the line width of the (002) peak increases and the corresponding peak intensity has a tendency to decrease with the increasing Cd

✉ Fax: +86-421-87952624, E-mail: dwm2002@163.com

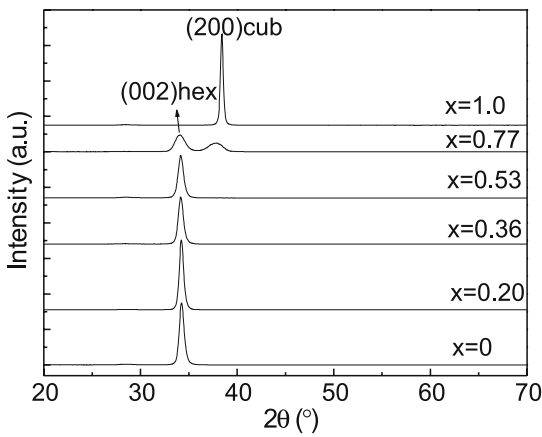


FIGURE 1 XRD spectra of $Zn_{1-x}Cd_xO/Si(111)$ thin films

content, except for the pure CdO film. The lattice parameter c calculated from the (002) peaks increases almost linearly from 5.229 Å ($x = 0$) to 5.247 Å ($x = 0.6$) and testifies that the substitution of the smaller Zn atom (with an ionic radius of 0.74 Å) by the larger Cd atom (with an ionic radius of 0.97 Å) takes place on the equivalent crystallographic position of Zn in the hexagonal wurtzite structure.

Normalized PL spectra taken at 12 K of all the samples are depicted in Fig. 2. A red shift of the near-band-edge (NBE) emission peaks with increasing Cd composition up to 53 at.%, as expected, can clearly be observed because of a smaller direct band gap of 2.3 eV of CdO than that of 3.3 eV of ZnO. Notably the line width of the peak increases, and the peak intensity and the shift magnitude of the peak position decrease gradually with the increasing Cd content, which were frequently observed in alloy semiconductors [11, 12]. It was considered that the Stokes shift is responsible for these phenomena, and the Stokes shift tends to become larger towards the Cd-rich direction, implying the gradually increased degree of composition fluctuation and structural disorder [12]. Continuing to increase the Cd content to 77 at.%, only very weak PL peaks likely arising from defects are observed, which is

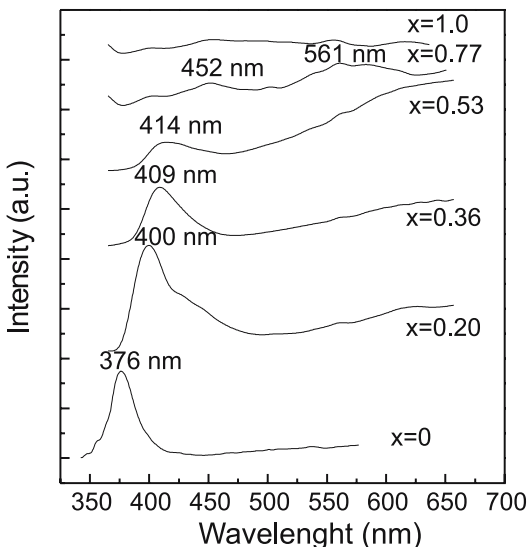


FIGURE 2 PL spectra of $Zn_{1-x}Cd_xO/Si(111)$ films measured at 12 K

consistent with the XRD results shown in Fig. 1, and, meanwhile, the film is a mixture of ZnO and CdO crystalline phases together with a mass of amorphous phase; therefore, the defect concentration in the film is so high that the PL behavior is seriously hampered. Pure CdO possesses no PL behavior, as was described elsewhere [13].

To further comprehend the PL mechanism of the alloy films, we now set out to analyze it from the viewpoint of band structure. According to Refs. [14, 15], a brief sketch map of the band structure of wurtzite ZnO is depicted in Fig. 3. The band-gap formation of ZnO is mainly caused by the interaction between the bonding valence-band orbital of $O2p$ and the antibonding conduction-band orbital of $Zn4s$. The neighboring $Zn3d$ orbital was also deemed as an important factor for the band-gap variation due to a $p-d$ interaction; it is said [14] that the action from this can push the $O2p$ orbital upward, therefore inducing the band gap of ZnO to become smaller. The $O2s$ and other core states are usually regarded as deep levels, which have relatively much smaller effects on the band-gap variation [14, 15]. Similarly, in view of the comparability between the Cd and Zn metals, the band structure of CdO is parallel to that of ZnO, which is illustrated in Fig. 3 and agrees with Ref. [16]. Here, for brevity, we can assume that the energies of the $O2s$ states in ZnO and CdO are both 0, while other states are omitted. It should be noted that the energy of the $Cd4d$ orbital is lower than that of the $Zn3d$ orbital, i.e. the $Cd4d$ orbital has a relatively much weaker effect on the variation of the CdO band gap than that of $Zn3d$ on ZnO. It is assumed that iso-molar ZnO and CdO react to form a perfect solid solution of wurtzite $ZnCdO_2$, that is, the O atoms in the alloy all possess the fourfold structures of $[OZn_2Cd_2]$. It was revealed [17] that no new states irrelevant to the original states are formed in an ideal iso-valent alloy (e.g. Zn and Cd are iso-valent, and both ZnO and CdO are II–VI), and instead the band edges move continuously with composition. Consequently, in the $ZnCdO_2$ alloy, a $Zn4s$ orbital and a $Cd5s$ orbital will give birth to two new hybrid orbitals of $Zn4s-Cd5s$, while $Zn3d$ and $Cd4d$ orbitals will produce two $Zn3d-Cd4d$ hybrid orbitals. And, the $O2p$ orbitals in ZnO and CdO will coalesce. Considering the intrinsic differences between the energies of the original orbital, the newly hybrid or coalescent energy levels of the orbitals will be widened. It can be reckoned that the NBE emissions of the $Zn_{1-x}Cd_xO$ ($x > 0$)

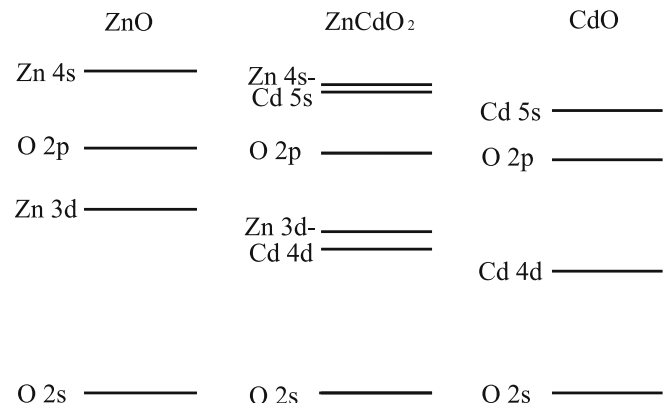


FIGURE 3 Schematic illustrations of band-gap structures of ZnO, CdO and iso-molar $ZnCdO_2$ alloy

films displayed in Fig. 2 are caused by radiative transitions between the $Zn4s$ – $Cd5s$ hybrid level and the $O2p$ level, and so the corresponding line widths of the PL peaks are larger than that of pure ZnO. On the other hand, with increasing Cd composition in $Zn_{1-x}Cd_xO$ films, the effect of a d orbital on the alloy band-gap variation gradually reduces, i.e. the resultant upward shift of the $O2p$ orbital decreases, and so the magnitude of the band-gap variation decreases, which accords with Fig. 2. For the actual iso-molar $ZnCdO_2$ alloy crystal, some disorders or defects always exist in it. For example, the O atom exists in the form of $[OZn_4]$, $[OCd_4]$, $[OZnCd_3]$ or $[OZn_3Cd]$, and other defects like V_O , Zn_i and Cd_i can also be found. Additionally, some chemical bonds may extend, shrink or twist. If these defect levels are close to the $O2p$ level or $Zn4s$ – $Cd5s$ hybrid level, or even coalescing with them, the orbital level is broadened, and then the line width of the PL spectrum is also widened. If the defect levels are far from the originally existing levels, i.e. some isolated levels form, luminescence from defects can be detected.

According to the above XRD and PL results, we can calculate c -axis constants and band gaps of the $Zn_{1-x}Cd_xO$ alloy films. Figure 4 shows the c -axis constant and band gap E_g of the $Zn_{1-x}Cd_xO$ ($0 \leq x \leq 0.53$) films as a function of Cd content x . Note that the relationship between the c -axis constant and the Cd content x accords with Végard's law, $c(x) = 0.5229 + 0.00357x$. However, the relationship between the band gaps E_g and the Cd contents x can be fitted using a quadratic equation, $E_g(x) = 3.30 - 1.22x + 1.26x^2$ ($0 \leq x \leq 0.53$), that is to say, a bowing parameter of 1.26 eV is evaluated for the wurtzite $Zn_{1-x}Cd_xO$ ($0 \leq x \leq 0.53$) alloys. The bowing parameter is usually deemed to come from three sources,

namely, the volume deformation, the chemical electronegativity difference and the internal structural relaxation [18].

4 Conclusion

In conclusion, we have proposed a new explanation from the viewpoint of band structure, which clearly elucidated the origin of the PL behaviors in $Zn_{1-x}Cd_xO$ alloys and may provide some profitable ideas for further investigating $Zn_{1-x}Cd_xO$ and other alloy semiconductors as applications in luminescent materials. In addition, a quadratic equation was put forward to depict the relationship between the band gaps E_g of the alloys and their Cd contents x , i.e. $E_g(x) = 3.30 - 1.22x + 1.26x^2$ ($0 \leq x \leq 0.53$). And, the relationship between the c -lattice parameter and the Cd content accords with Végard's law, $c(x) = 0.5229 + 0.00357x$. The investigations show that the $Zn_{1-x}Cd_xO$ alloy films will have great potential in the applications of short-wavelength optoelectronic devices.

ACKNOWLEDGEMENTS This work was supported by the Natural Science Foundation of the Education Ministry of Zhejiang Province of China under Grant No. G20408 and the Korean Research Foundation under Grant No. KRF-2004-005-C0041.

REFERENCES

- 1 R.F. Service, *Science* **276**, 895 (1997)
- 2 W.I. Park, S.J. An, G.C. Yi, H.M. Jang, *J. Mater. Res.* **16**, 1358 (2001)
- 3 T. Gruber, C. Kirchner, R. Kling, F. Reuss, A. Waag, F. Bertram, D. Forster, J. Christen, M. Schreck, *Appl. Phys. Lett.* **83**, 3290 (2003)
- 4 H. Tabet-Derraz, N. Benramdane, D. Nacer, A. Bouzidi, M. Medles, *Sol. Energy Mater. Sol. Cells* **73**, 249 (2002)
- 5 O. Vigil, L. Vaollant, F. Cruz, G. Santana, A. Moroles-Acevedo, G. Contreras-Puente, *Thin Solid Films* **361–362**, 53 (2000)
- 6 Y.S. Choi, C.G. Lee, S.M. Cho, *Thin Solid Films* **289**, 153 (1996)
- 7 G. Torres-Delgado, C.I. Zuniga-Romero, O. Jimenez-Sandoval, R. Castanedo-Perez, B. Chao, S. Jimenez-Sandoval, *Adv. Funct. Mater.* **12**, 129 (2002)
- 8 K. Sakurai, T. Takagi, T. Kubo, D. Kajita, T. Tanabe, H. Takasu, S. Fujita, S. Fujita, *J. Cryst. Growth* **237–239**, 514 (2002)
- 9 T. Makino, Y. Segawa, M. Kawasaki, A. Ohtomo, R. Shiroki, K. Tamura, T. Yasuda, H. Koinuma, *Appl. Phys. Lett.* **78**, 1237 (2001)
- 10 D.W. Ma, Z.Z. Ye, H.M. Lu, J.Y. Huang, B.H. Zhao, L.P. Zhu, H.J. Zhang, P.M. He, *Thin Solid Films* **461**, 250 (2004)
- 11 A. Ohtomo, M. Kawasaki, T. Koida, K. Masubuschi, K. Koinuma, Y. Sakurai, Y. Yoshida, T. Yasuda, Y. Segawa, *Appl. Phys. Lett.* **72**, 2466 (1998)
- 12 J. Wu, W. Walukiewicz, K.M. Yu, J.W. Ager III, E.E. Haller, H. Lu, W.J. Schaff, *Appl. Phys. Lett.* **80**, 4741 (2002)
- 13 A.B.M.A. Ashrafi, H. Kumano, I. Suemune, Y.W. Ok, T.Y. Seong, *Appl. Phys. Lett.* **79**, 470 (2001)
- 14 P. Schroer, P. Kruger, J. Pollmann, *Phys. Rev. B* **47**, 6971 (1993)
- 15 M. Usuda, N. Hamada, *Phys. Rev. B* **66**, 125 101 (2002)
- 16 R.J. Guerrero-Moreno, N. Takeuchi, *Phys. Rev. B* **66**, 205 205 (2002)
- 17 J.A. van Vechten, T.K. Bergstresser, *Phys. Rev. B* **1**, 3351 (1970)
- 18 J.E. Bernard, A. Zunger, *Phys. Rev. B* **36**, 3199 (1987)

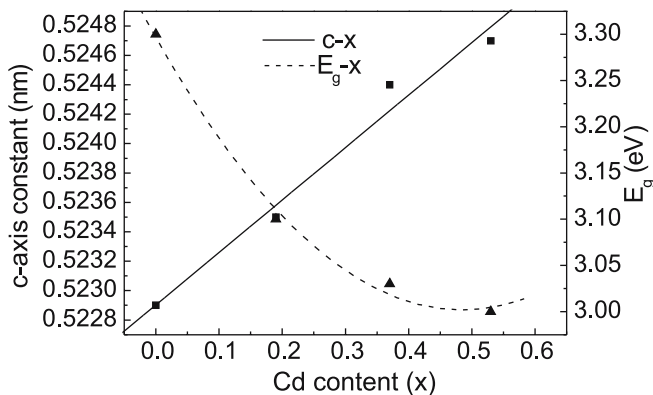


FIGURE 4 The c -axis constant and band gap E_g of $Zn_{1-x}Cd_xO$ ($0 \leq x \leq 0.53$) films as a function of Cd content x